The mechanism of fast Ni diffusion in the high-temperature phase of Ni_3Sb studied with quasielastic neutron scattering

1996 J. Phys.: Condens. Matter 8 4727

(http://iopscience.iop.org/0953-8984/8/26/005)

J. Phys.: Condens. Matter **8** (1996) 4727–4738. Printed in the UK

The mechanism of fast Ni diffusion in the high-temperature phase of Ni_3Sb studied with quasielastic neutron scattering

G Vogl†, M Kaisermayr† and O G Randl‡

† Institut für Festkörperphysik der Universität Wien, A-1090 Wien, Austria
‡ Institut Laue–Langevin, F-38042 Grenoble, France

Received 22 January 1996, in final form 27 March 1996

Abstract. Nickel diffusion in Ni_3Sb ($D0_3$ structure, four sublattices) is so fast that an unusual jump mechanism might be suspected. This suspicion is nourished by the recent discovery of high concentrations of ordered vacancies, i.e. vacancies on two of the nickel sublattices, the α-sublattices. Quasielastic neutron scattering (QNS) can be used to determine the elementary diffusion jump. Using this method we have found that the elementary diffusion jump is unambiguously a jump into a nearest-neighbour site, i.e. between sites on α- and γ-sublattices. In spite of the very high vacancy concentration on the α-sites (which certainly supports the fast jumping) it is—interestingly enough—not a jump directly between α-sites.

1. Introduction

An interesting feature of some intermetallic alloys (or just 'intermetallics') is the extraordinarily high diffusivity of one of the constituents. It seems to be a general property of $D0_3$ intermetallics that the diffusion of the majority component is much faster than that of the minority component, and also considerably higher than diffusion in other intermetallics (Wever *et al* 1989). The elementary diffusion process in several intermetallics has therefore been the subject of recent studies. Quasielastic Mössbauer spectroscopy (QMS) has served to determine the elementary diffusion jump of Fe atoms in the system Fe–Si at compositions around Fe_3Si (Sepiol and Vogl 1993, 1995) and in the system Fe–Al in the range from 50 at.% Fe to 75 at.% Fe (Vogl and Sepiol 1994, Feldwisch *et al* 1995). With quasielastic neutron scattering (QNS; see, e.g., Bée 1988) the elementary jump of Ni atoms in hcp NiSb has been determined (Vogl *et al* 1993).

Here we report on a QNS study of Ni diffusion in the high-temperature β-phase of the intermetallic $Ni_{72.5}Sb_{27.5}$. According to the phase diagram (Heinrich *et al* 1978) the alloy melts congruently at that composition, and not at the stoichiometric composition $Ni_{75}Sb_{25}$. Therefore even though growth with the floating-zone method produces crystals close to $Ni_{72.5}Sb_{27.5}$ (the crystals that we have used), in the following for the sake of brevity we shall call the alloy Ni_3Sb. The crystal structure is the cubic $D0_3$ structure (figure 1), space group $Fm\bar{3}m$, that phase being stable above 530 °C. On a temperature scale reduced to the melting temperature (figure 2) Ni atoms exhibit the fastest self-diffusion ever observed in an intermetallic alloy—to the best of our knowledge even the fastest self-diffusion of metal atoms ever observed in a purely metallic system. Heumann and Stüer (1966) have shown that the Ni diffusivity increases with the departure from the stoichiometric composition, which gave rise to the assumption of fast diffusion induced by off-stoichiometric vacancies

0953-8984/96/264727+12$19.50

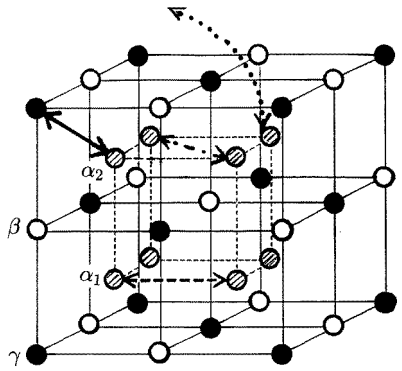

Figure 1. The $D0_3$ structure can be interpreted as a bcc lattice with a superstructure in the form of an alternate occupation of the centred sites by Ni and Sb atoms. The lattice can be seen as being composed of four individual fcc sublattices. In Ni_3Sb three of them (α_1, α_2, both hatched circles, and γ, full circles) are occupied by Ni atoms, and one (β, open circles) is occupied by Sb atoms. The different arrows symbolize the different jump models discussed in section 5.

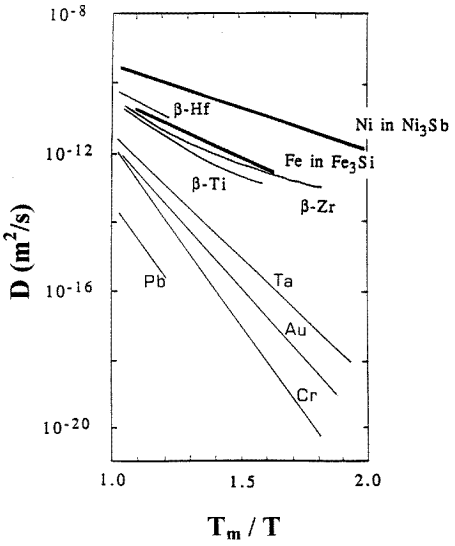

Figure 2. A comparison of self-diffusion rates of selected metals and intermetallics on a reduced temperature scale.

on Ni sites. Measurements of the electrotransport in Ni_3Sb performed by the same authors suggest that the Ni diffusion exceeds that of Sb by several orders of magnitude (Heumann and Stüer 1967).

Indeed, vacancies were found in powder diffraction measurements on various alloys in the composition range from $Ni_{71}Sb_{29}$ to $Ni_{75}Sb_{25}$ (Randl 1994, Randl *et al* 1996) by measuring the elastic coherent neutron scattering, in particular the intensities of the (111) and (200) reflections. The vacancies are found not to be distributed in equal fractions on all Ni sublattices, but rather to be concentrated on the α-sublattices. On the β-sublattice no antistructure Ni atoms could be detected, that lattice obviously belonging exclusively to the Sb atoms. Moreover one would not expect the Ni atoms to use vacancies on regular Sb sites much more often than the Sb atoms themselves with their lower diffusivity.

Therefore we exclude the possibility of Ni jumps via β-sites (normally occupied by Sb atoms). Considering the high vacancy concentrations on the α-sites there appear to be various possible jump models for Ni atoms:

(i) jumps exclusively between α-sites, possibly even over large distances (which would make the extremely high diffusivity plausible); and

(ii) jumps between α- and γ-sites, i.e. nearest-neighbour (NN) sites.

2. Elementary jump processes studied with quasielastic neutron scattering

QNS and QMS are two competing tools for the examination of lattice diffusion mechanisms (jump length and jump vector) on an atomic scale. A comparison of these methods has been given by Petry and Vogl (1987) and by Vogl (1996). While coherent neutron scattering yields information about collective phenomena, incoherent neutron scattering is sensitive to the movement of a *single* atom. In our case, QNS is ideal as there exist no appropriate isotopes for Mössbauer spectroscopy and the relevant incoherent neutron scattering length of Ni (5.3 b) is quite sufficient and exceeds by far that of Sb (0.3 b) (Sears 1984). Therefore Sb is practically invisible as regards incoherent neutron scattering.

Besides quasielastic incoherent scattering there is quasielastic coherent diffuse scattering (Ross and Wilson 1978). We have earlier discussed the problems associated with the overlap of the two in the case of a NiSb alloy (Vogl *et al* 1993). In the presence of vacancies on the Ni sublattices diffuse coherent scattering of Laue type is proportional to the coherent scattering cross section of the Ni atoms (13.3 b, Sears 1984) and to the product of the concentrations of Ni atoms and vacancies. The corresponding cross section for, say, 10% vacancies on the Ni sublattices is then about 20% of the incoherent cross section of the Ni atoms. In the case of a correlation of the diffusing atoms or relaxation of the surrounding atoms whilst an atom is undergoing a jump between lattice sites, according to Sinha and Ross (1988) short-range-order diffuse scattering would come into play. Measurements of diffuse short-range-order scattering which are under way for intermetallic alloys could yield information on the amount of diffuse scattering and could enable an estimate of its contribution to quasielastic scattering to be obtained, but in default of such information for the time being we have to neglect such a possible contribution in the evaluation of the present data.

The individual movements of the atoms—jumps in the case of a lattice—lead to a broadening of the elastic incoherent intensity in energy space, called quasielastic line broadening. Since this broadening is weak, exceptionally high energy resolution is necessary. Apart from Mössbauer spectroscopy only spin-echo and neutron backscattering spectrometers provide sufficient resolution to study diffusivities as low as 10^{-11} m^2 s^{-1}. The theory relating the elementary jump process and linewidth (Singwi and Sjölander 1960) is rather simple in the case of NN jumps in a Bravais lattice (Chudley and Elliott 1961). It yields a dependence on momentum ($\boldsymbol{Q}$) and energy ($\hbar\omega$) of the incoherent scattering function in the form of a Lorentzian line which, except for trivial normalization, is

$$S(\boldsymbol{Q},\omega) = \frac{\Gamma(\boldsymbol{Q})/2}{[\Gamma(\boldsymbol{Q})/2]^2 + \omega^2} \tag{1}$$

with a linewidth (FWHM) corresponding to the diffusional line broadening

$$\Gamma = \frac{2\hbar}{\tau}\left[1 - (1/N)\sum_{\boldsymbol{k}} \exp(\mathrm{i}\boldsymbol{Q}\cdot\boldsymbol{l}_k)\right] \tag{2}$$

where N is the number of NN atoms, $\boldsymbol{l}_k$ denotes the kth jump vector, and τ is the residence time between two jumps (the jump time itself is considered to be negligibly short).

In the case of non-Bravais lattices (as, e.g., in the $D0_3$ lattice) the theory becomes more complicated (Rowe *et al* 1971, Kehr *et al* 1978, Anderson *et al* 1984, Richter *et al* 1991). A detailed derivation and a comparison of QNS and QMS has recently been given by Randl *et al* (1994). The generalized form of equation (1) including jumps via various sublattices is

$$S(\boldsymbol{Q},\omega) = \sum_p w_p(\boldsymbol{Q}) \frac{\Gamma_p(\boldsymbol{Q})/2}{[\Gamma_p(\boldsymbol{Q})/2]^2 + \omega^2} \tag{3}$$

where p is the number of different sublattices involved in the jump process. In the case of nearest-neighbour jumps on a $D0_3$ lattice, p equals four, and consequently the number of Lorentzians that sum up to the scattering law is four. The linewidths (FWHM) of the Lorentzians (again describing the diffusional line broadening) are the eigenvalues of a matrix $\mathbf{A}$ which we call the jump matrix. It has components

$$A_{ij} = \frac{1}{n_{ji}\tau_{ji}} \sum_k \exp(\mathrm{i}\boldsymbol{Q}\cdot\boldsymbol{l}_{ij}^k) - \delta_{ij} \sum_j \frac{1}{\tau_{ij}}. \tag{4}$$

Here we have assumed that each site on the ith sublattice is surrounded by n_{ij} sites on the jth sublattice, the kth of which is at a vector distance $\boldsymbol{l}_{ij}^k$. τ_{ij} is the residence time at a site of symmetry i before the jump occurs to any NN site of symmetry j. The weights of the Lorentzian components are related to the eigenvectors of the hermitized matrix. δ_{ij} is one for $i = j$ and zero otherwise.

3. Preparation and orientation of the samples

The measurements were performed on single crystals of Ni_3Sb in the form of rods of 36 mm length and about 8 mm diameter. The crystals had been grown by the floating-zone technique. While the crystal of the first measuring series was grown directly in the measuring furnace and received no further containment, the crystal of the second series was fixed in a cylinder made out of 60 μm thick Nb sheet and then placed in the furnace. The furnace was mounted on the backscattering spectrometer IN10 of the ILL (Ibel 1994).

The crystals were oriented at the three-axis spectrometer IN3 of the ILL. Since the $D0_3$-structured β-phase of Ni_3Sb is stable above 530 °C only, the orientation had to be performed at high temperature. Previous experiments on Ni_3Sb single crystals concerning the phase transition between the low- and high-temperature phases had shown that the orientation does not change when the crystal is cooled below the phase transition and reheated again, though after repeated cycling the crystal quality decreases. In order to prevent any risks regarding crystal quality and orientation we did not cool the crystals between orientation and QNS measurements but rather transferred the hot furnace containing the crystal from IN3 to IN10.

4. Experiment and data treatment

Measurements were performed in two series, one just before a four-year stop of the ILL reactor, the other soon after its restart.

In the first series, the QNS was measured in three different crystal orientations, namely $\langle 60, 5, 135\rangle$, $\langle 90, 5, 135\rangle$, and $\langle 120, 5, 135\rangle$, with Euler angles $\langle \Phi, \Theta, \Psi\rangle$ in degrees as defined by Goldstein (1980). The nominal sample temperatures were 800 °C and 700 °C,

the latter only for ⟨60, 5, 135⟩. The individual orientations were obtained by turning the furnace in the horizontal plane. Each of the four measurements took about one day. In addition a measurement with a vanadium sample made in order to determine the resolution of the instrument and an 'empty-can measurement' to account for the scattering of the empty furnace were performed. We used the backscattering spectrometer IN10 in its original version IN10A. The wavelength of incoming neutrons was 6.27 Å, Q-values were between 0.27 and 1.94 $Å^{-1}$, the energy resolution was 1 μeV, and the energy range was ± 12 μeV. As will be discussed, the expected Lorentzians with large diffusional broadening were inaccessible in this experiment. We have given a short preliminary report on the results (Sepiol *et al* 1994).

In the second measuring series three crystal orientations (⟨110, 8, 258.5⟩, ⟨140, 8, 258.5⟩, and ⟨170, 8, 258.5⟩) were scanned at nominally 690 °C, the first two also at 780 °C. To improve counting statistics compared to the former measurement series we spent 45 hours on each measurement and 21 hours on each of two resolution runs and the empty-can measurement. The positioning of the eight detectors allowed us to take spectra at Q-values between 0.41 $Å^{-1}$ and 1.93 $Å^{-1}$. To avoid the risk of contamination by (111) Bragg reflections (coherent scattering) from possibly misoriented grains at the surface of the crystal, we covered the analyser plates with a cadmium sheet in the angular range where this reflection could appear, i.e. between 130 and 138°. Higher Bragg reflections are outside the angular range of IN10 and cannot disturb the measurements. We performed two resolution measurements, one with vanadium and one with the sample itself, both at room temperature where no diffusion-induced line broadening occurs.

This measurement series was performed on the new version of the IN10 backscattering spectrometer named IN10B. The principle was as follows: in order to vary the energy of the incoming neutrons (wavelength again 6.27 Å) a KCl monochromator in the (200) position was cooled down to about -180 °C and slowly reheated to about 130 °C during each measurement (Cook *et al* 1992). The change in lattice constant obtained in that way provided an energy difference from -13 μeV to 40 μeV between incoming neutrons and those which fulfil the backscattering condition of the Si(111) analyser plates. In principle much larger energy transfers would be possible at IN10B, but for our purposes 40 μeV was sufficient. This high energy range proved to be necessary to fully scan the broader part of the QNS spectra at temperatures well in the existence range of the β-phase. Since there is practically no quasielastic intensity above 40 μeV, we were able to perform a reliable background subtraction and determine the width of the broader line as well. The drawback of the version IN10B was its weaker energy resolution of 3 μeV compared to 1 μeV at IN10A.

Figure 3 compares two typical spectra obtained at the IN10A and the IN10B.

The raw data were treated with the routine SQW available at the ILL which subtracts background and carries out absorption corrections. Fits with one as well as with two Lorentzians were carried out using the ILL routine WLL.

5. Models for the elementary jump process

5.1. Jumps exclusively between α-sites

Figure 4 shows the linewidths (FWHM) due to diffusional broadening (i.e. the full experimental widths deconvoluted by the instrumental resolution) for the three crystal orientations and two temperatures of the second measuring series, together with various model curves. The experimental data have been gained from fits of the spectra with just

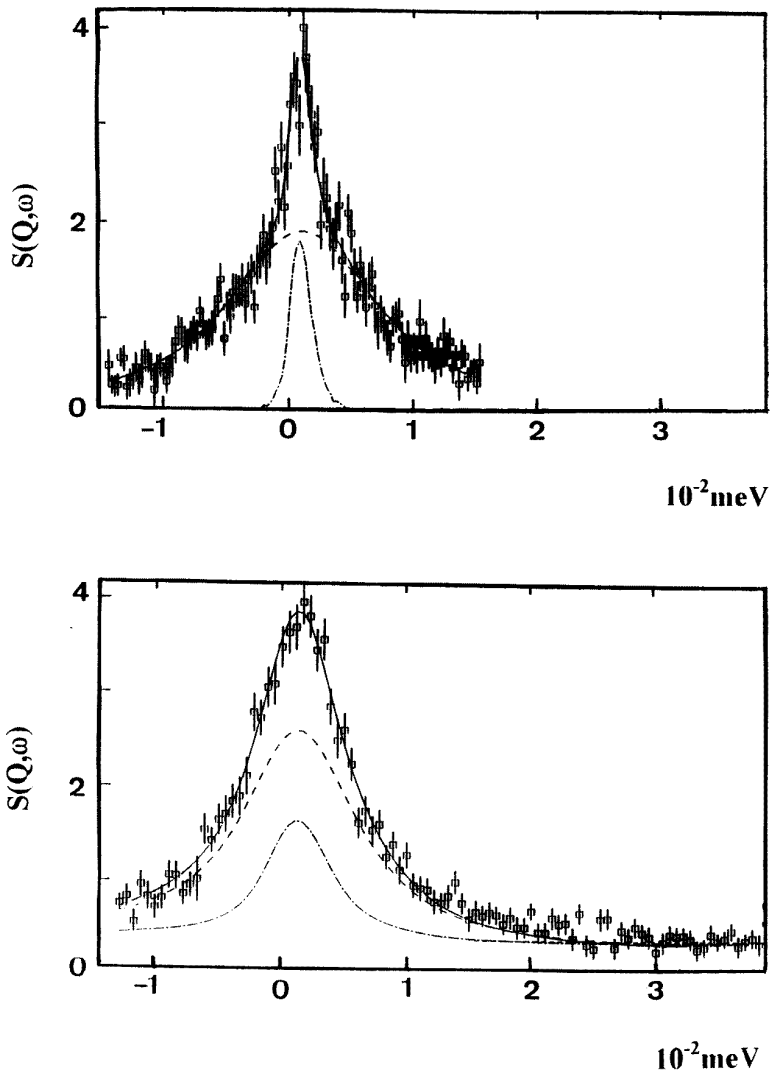

Figure 3. The quasielastic scattering intensity $S(Q, \omega)$ in arbitrary units as a function of energy. Top: IN10A, 800 °C (Sepiol *et al* 1994); bottom: IN10B, 780 °C; both at about $Q = 1.8$ Å^{-1}. Notice that at 15 μeV (the limit of IN10A) there is still non-negligible quasielastic intensity belonging to the broader Lorentzian—therefore a correct consideration of the background was impossible, and the background was arbitrarily set to zero; whereas the curve has reached the background at 40 μeV (the maximum energy transfer in the experiment on IN10B).

one Lorentzian line, i.e. with the Chudley–Elliott model for jumps on a Bravais lattice.

As mentioned above, the high vacancy concentration on the α-sublattices suggests models which are based on jumps between α-sites exclusively. Several jump mechanisms of this kind will be discussed.

(a) Jumps between far distant α-sites. One could naively assume that the unusually high Ni diffusivity in Ni_3Sb is due to long jumps of the Ni atoms directly into rather far

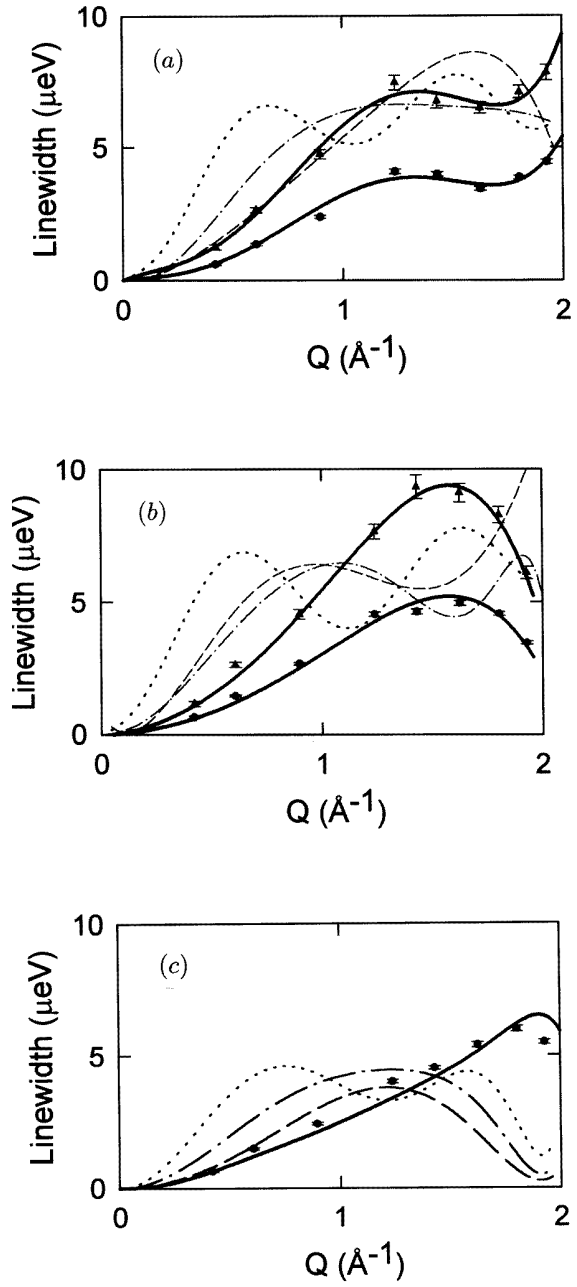

Figure 4. (a), (b) and (c): crystal orientations $\langle \Phi, \Theta, \Psi \rangle = \langle 110, 8, 258.5 \rangle$, $\langle 140, 8, 258.5 \rangle$, and $\langle 170, 8, 258.5 \rangle$. A comparison is shown between measured diffusional line broadenings, FWHM (fits with one broadened line only), at $T = 690$ °C (dots) and 780 °C (triangles), and the linewidths as calculated with the assumptions of various jump models, namely: (1) jumps exclusively between α-sites (a) at large distances (quite arbitrarily a distance of three times the lattice parameter a was chosen)—dotted lines; (b) at the distance $a/\sqrt{2}$, i.e. across the face diagonal of the cube formed by the α-sites—dash-dotted lines; and (c) at the distance $a/2$, i.e. along the edges of the α-site cube—dashed lines; and (2) jumps between α- and γ-sites at the distance $(a\sqrt{3})/4$ (nearest neighbours), i.e. across half of the body diagonal of the α-site cube. The width is a weighted average of three lines according to equation (9)—thick lines.

distant neighbour sites. Let us see how the experiments agree with such a hypothesis. In figure 4 the dotted lines represent Chudley–Elliott model predictions according to equation (2) for jumps over a distance of three times the lattice parameter $a = 5.93$ Å. It is evident that there is no way to reconcile model and experiment: the first maximum in the theory appears at a small Q-value where the experimental data still increase with increasing Q. The naive hypothesis of direct jumps into distant neighbours can therefore be excluded.

(b) Jumps via the face diagonal of the α-cube. As this model presumes only jumps between sites either of the α_1- or the α_2-sublattices, but no jumps between these two lattices, we can regard them as NN jumps between equivalent sites on an fcc lattice and again apply the Chudley–Elliott theory, which yields the Q-dependence of the linewidth after inserting the jump vectors into equation (2). It is evident from figure 4 that the Q-dependences of the calculated linewidths (dash-dotted lines) again have no similarity to the diffusional line broadenings found in the experiment, so jumps of this kind can also be excluded.

(c) Jumps between α-sites along the edge of the cubic unit cell. As these jumps correspond to NN jumps between equivalent sites on the simple cubic lattice of the α-sites, again the Chudley–Elliott theory for Bravais lattices can be applied. From equation (2) one obtains for the linewidths the curves as shown in figure 4 as dashed lines. As there is again no agreement between model predictions and experimental data, this process again can be excluded.

5.2. Jumps between α-and γ-sites, i.e. to nearest-neighbour sites

To calculate linewidths in the case of NN jumps we have to employ the theory for non-Bravais lattices, since the sites are inequivalent. As described in section 2, this leads to more than one Lorentzian and they are all centred around zero energy transfer but with different widths. For the $D0_3$ structure in the most general case we expect four Lorentzians because of the four inequivalent sites in the unit cell. Their widths correspond to the eigenvalues of a 4×4 jump matrix (equation (4)). The four eigenvalues have to be calculated numerically.

It would be a hopeless endeavour to attempt a fit of four Lorentzian lines with different widths to data with an experimental resolution of the order of these widths. Fortunately we know from the powder diffraction data (Randl 1994, Randl *et al* 1996) that Ni atoms avoid β-sites, the latter being occupied by the Sb atoms only. Thus we are left with three Ni sites in the $D0_3$ unit cell and therefore three Lorentzian lines which correspond to the eigenvalues of a 3×3 jump matrix.

According to equation (4), matrix $\mathbf{A}$ has the diagonal terms $-2/\tau_{\gamma\alpha}, -1/\tau_{\alpha\gamma}, -1/\tau_{\alpha\gamma}$ where $\tau_{\gamma\alpha}$ and $\tau_{\alpha\gamma}$ are the residence times on sites of the two types of Ni sublattice, the γ-sublattice and the α-sublattice, respectively, before the jump to a site on the other Ni sublattice occurs. The off-diagonal terms are functions of the structure of the 'jump lattice', i.e. the lattice which is visited by the Ni atoms on jumping, and contain a 'structure factor'

$$E = \cos(Q_x a)\cos(Q_y a)\cos(Q_z a) + \mathrm{i}\sin(Q_x a)\sin(Q_y a)\sin(Q_z a). \tag{5}$$

The matrix reads

$$\mathbf{A} = \begin{pmatrix} -2/\tau_{\gamma\alpha} & E/\tau_{\alpha\gamma} & E^*/\tau_{\alpha\gamma} \\ E^*/\tau_{\gamma\alpha} & -1/\tau_{\alpha\gamma} & 0 \\ E/\tau_{\gamma\alpha} & 0 & -1/\tau_{\alpha\gamma} \end{pmatrix}. \tag{6}$$

While the eigenvalues of the 4×4 matrix $\mathbf{A}$ have to be calculated numerically, there is an analytical solution for the 3×3 matrix. The negative eigenvalues are the half-widths (HWHM = (1/2)FWHM). One of the eigenvalues is independent of the structure factor E

and therefore of crystal orientation relative to the neutron beam:

$$M_1 = -1/\tau_{\alpha\gamma}. \tag{7}$$

The two other eigenvalues are

$$M_{2,3} = -(1/4\tau_{\gamma\alpha})[2f + 4 \pm \sqrt{(2f-4)^2 + 2fEE^*}] \tag{8}$$

with $f = \tau_{\gamma\alpha}/\tau_{\alpha\gamma}$.

The weights are related to the eigenvectors (see Randl *et al* 1994); their numerical values may be found in Randl (1994).

As reported by Sepiol *et al* (1994), the experiment on IN10A was in agreement with the predictions of this model. However, the insufficient energy range made the determination of the background and, in consequence, that of the width of the broad component impossible. Therefore, competing models could not be excluded.

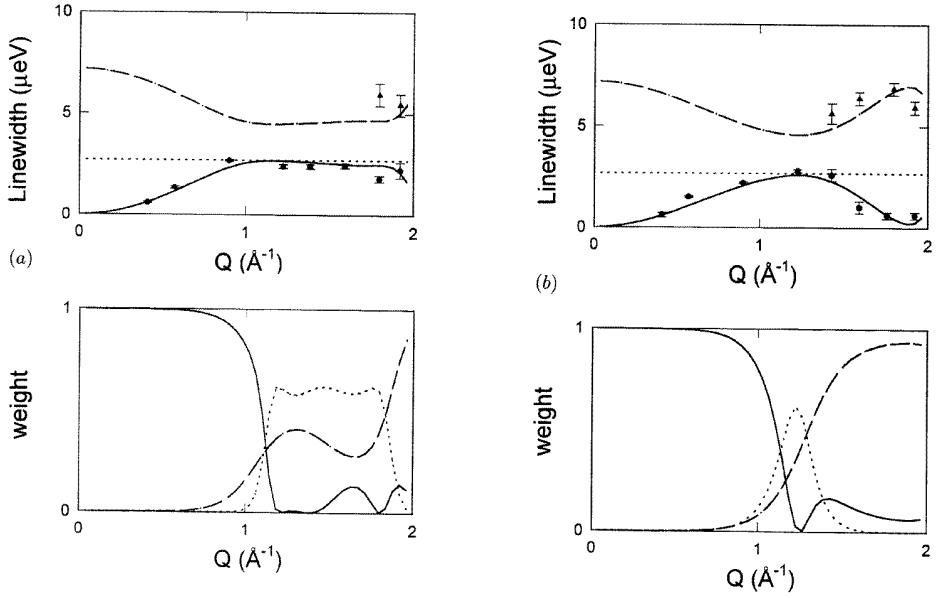

Figure 5. (*a*) and (*b*): crystal orientations $\langle \Phi, \Theta, \Psi \rangle = \langle 110, 8, 258.5 \rangle$ and $\langle 170, 8, 258.5 \rangle$; $T = 690\ ^\circ$C. Top panels: dots and triangles: diffusional line broadenings (FWHM) from a fit of the measured spectra with two Lorentzians; curves: theoretical linewidths (FWHM) according to the three-Lorentzian model for jumps between α- and γ-sites. The fit values for the broad line were reliable only when the weight of the broad line was above about 50% or when the linewidths differed sufficiently. Therefore in (*a*) no values for the widths of the broad line are given below 1.8 Å^{-1} and in (*b*) no values for the widths of the broad line are given below 1.4 Å^{-1}. The component underlying the dotted curve has significant weight only when its width coincides with that of the narrow line; this is why a three-Lorentzian fit of the data is not necessary. Bottom panels: relative weights of Lorentzians according to the model.

The situation was improved in the second measuring series. Now the energy range was wide enough to allow full separation of the broad line from the background. Figure 5(*a*) shows as an example linewidths and weights for the crystal orientation $\langle \Phi, \Theta, \Psi \rangle = \langle 110, 8, 258.5 \rangle$, and figure 5(*b*) is for the orientation $\langle \Phi, \Theta, \Psi \rangle = \langle 170, 8, 258.5 \rangle$.

It is evident that *de facto* only two instead of three lines have to be considered when comparing with measurements, since the line whose width is independent of Q has reasonable weight only when its width approaches that of the narrower line. Therefore the weights of the two lines can always be added, and the experimental values be compared with two lines, a narrow and a broad one.

The data points in figures 5 (top panels) show the linewidths for fits of the spectra with two lines. Two-line fits were not straightforward; we had to fix the relative weights of the two lines while running the fit. To compare experimental data with theory we imposed the weights predicted for a certain model and compared the fitted diffusional line broadenings with the linewidths expected for this model.

The agreement with the model is satisfactory. A completely free fit (with both widths and weights free) is beyond the resolution of the measurement, but might perhaps be promising if the instrumental resolution could be improved to better than 1 μeV.

We have also determined weighted averages of the three lines

$$\Gamma = w_1\Gamma_1 + w_2\Gamma_2 + w_3\Gamma_3 \tag{9}$$

and have plotted them as thick lines in figure 4. Their analytical shapes agree excellently with the values derived from one-line fits to the experimental data.

From the fitted absolute values of the linewidths the atomic jump rate is derived; it is different for the two different temperatures which in the figures are symbolized by dots and triangles. The dependence of the diffusional line broadening (full width at half-maximum, FWHM) on the wave number Q at small Q (hydrodynamic or continuum limes) yields diffusivities according to

$$\lim \Gamma(Q \to 0) = 2\hbar D Q^2. \tag{10}$$

As the smallest value for Q measured in our experiment was 0.41 Å^{-1}, we used the line broadenings at small Q from the theoretical curves that we fitted to our data. This procedure is justified by the fact that the Q-dependence of the linewidths for small momentum transfer is independent of the assumed model and orientation. We obtained the following diffusivities:

$$D(690\ ^\circ\mathrm{C}) = 3.0(4) \times 10^{-11}\ \mathrm{m^2\ s^{-1}}$$
$$D(780\ ^\circ\mathrm{C}) = 5.4(6) \times 10^{-11}\ \mathrm{m^2\ s^{-1}}.$$

From Heumann and Stüer (1966) we derive values of D between 2×10^{-11} m^2 s^{-1} and 3×10^{-11} m^2 s^{-1} at 690 °C and between 4×10^{-11} m^2 s^{-1} and 5×10^{-11} m^2 s^{-1} at 780 °C for Ni concentrations in the range between 72.9 and 71.7 at.%. Determination of diffusivities is the domain of tracer measurements, and the diffusivities determined by that method are considerably more precise than those determined using QNS, the domain of the latter method being the determination of the elementary diffusion jump. The agreement between diffusivities derived from tracer and from QNS data is, however, satisfactory.

Finally we compare the self-diffusion of Fe atoms in Fe_3Si, another intermetallic with $D0_3$ structure which we have studied recently with quasielastic Mössbauer spectroscopy (QMS), finding that also there the elementary diffusion jump of the Fe atoms is a jump between α- and γ-sublattices (Sepiol and Vogl 1993, 1995). Also in this system, the diffusivity of iron on a reduced temperature scale (figure 2) is much higher than that in most elementary metals even though it is not as high as for Ni in Ni_3Sb, and again a high vacancy concentration is supposed to be the reason.

6. Conclusion

The NN-jump model offers excellent agreement with the experimental data, while models based on jumps other than between nearest neighbours can be excluded. Making use of our knowledge about occupancies on the different sublattices we explain the Ni diffusion as follows: jumps between regular Ni sites, profiting from the high vacancy concentration on two of the three Ni sublattices.

Again—as in nearly all of our investigations of the elementary diffusion jump—we have found a jump into a nearest-neighbour site. This might appear tedious, but—to turn the tables—it reconfirms that for jumps on lattices it is obviously energetically considerably cheaper to perform a short jump, i.e. a NN jump, than a jump to a more distant neighbour, even if that latter jump is only a few per cent longer. In other words: the energy barrier to overcome the saddle point is considerably higher if the jump length is only a few per cent larger. Even in the present case, which represents to the best of our knowledge the fastest self-diffusion of metal atoms in purely metallic systems ever measured, the elementary diffusion jump is not a jump over a great distance (which would appear possible because of the extremely high vacancy concentration); it is instead again a jump just into a vacancy on a NN site.

Acknowledgments

One of us (GV) is indebted to H Wever for directing his interest to diffusion in the system Ni_3Sb. GV is grateful to the Institut Laue–Langevin for the opportunity of spending a sabbatical there. We thank B Sepiol for a number of enlightening discussions, and W Henggeler for help with the crystal orientation. This work was financed by the Austrian Fonds zur Förderung der Wissenschaftlichen Forschung (FWF), contract S5601.

References

Anderson I S, Heidemann A, Bonnet J E, Ross D K, Wilson S K and McKergow M 1984 *J. Less-Common Met.* **101** 405
Bée M 1988 *Quasielastic Neutron Scattering* (Bristol: Hilger)
Chudley C T and Elliott R J 1961 *Proc. Phys. Soc.* **77** 353
Cook J C, Petry W, Heidemann A and Barthélemy J-F 1992 *Nucl. Instrum. Methods* A **312** 553
Feldwisch R, Sepiol B and Vogl G 1995 *Acta Metall. Mater.* **43** 2033
Goldstein H 1980 *Classical Mechanics* 2nd edn (Reading, MA: Addison-Wesley)
Heinrich S, Rexer H U and Schubert K 1978 *J. Less-Common Met.* **60** 65
Heumann T and Stüer H 1966 *Phys. Status Solidi* **15** 95
——1967 *Z. Naturf.* a **22** 1184
Ibel K 1994 *The Yellow Book* (Grenoble: Institut Laue–Langevin)
Kehr K W, Richter D and Swendsen R H 1978 *J. Phys. F: Met. Phys.* **8** 433
Petry W and Vogl G 1987 *Mater. Sci. Forum* **15–18** 323
Randl O G 1994 *Thesis* Universität Wien
Randl O G, Sepiol B, Vogl G, Feldwisch R and Schroeder K 1994 *Phys. Rev.* B **49** 8768
Randl O G, Vogl G, Bührer W, Kaisermayr M, Pannetier P and Petry W 1996 *J. Phys.: Condens. Matter* to be submitted
Richter D, Hempelmann R and Schönfeld C 1991 *J. Less-Common Met.* **172–174** 595
Ross D K and Wilson D L T 1978 *Neutron Inelastic Scattering* vol 2 (Vienna: IAEA) p 383
Rowe J M, Sköld K and Flotow H E 1971 *J. Phys. Chem. Solids* **32** 41
Sears V F 1984 *Chalk River Nuclear Laboratories Report* AECL-8490
Sepiol B, Randl O G, Karner C, Heiming A and Vogl G 1994 *J. Phys.: Condens. Matter* **6** L43
Sepiol B and Vogl G 1993 *Phys. Rev. Lett.* **71** 731

Sepiol B and Vogl G 1995 *Hyperfine Interact.* **95** 149
Singwi K S and Sjölander A 1960 *Phys. Rev.* **119** 863
Sinha S K and Ross D K 1988 *Physica* B **149** 51
Vogl G 1996 *Physica* B at press
Vogl G, Randl O G, Petry W and Hünecke J 1993 *J. Phys.: Condens. Matter* **5** 7215
Vogl G and Sepiol B 1994 *Acta Metall. Mater.* **42** 3175
Wever H, Hünecke J and Frohberg G 1989 *Z. Metallk.* **80** 389